

This is the **accepted version** of the journal article:

Aghamohammadi, Mahdiah; Fernández, Anton; Schmidt, Malte; [et al.]. «Influence of the relative molecular orientation on interfacial charge-transfer Excitons at donor». Journal of physical chemistry. C, Vol. 118, Num. 27 (June 2014), p. 14833-14839. DOI 10.1021/jp5041579

This version is available at <https://ddd.uab.cat/record/275376>

under the terms of the  ^{IN} COPYRIGHT license

Influence of the Relative Molecular Orientation on Interfacial Charge Transfer excitons at Donor/Acceptor Nanoscale Heterojunctions

*Mahdieh Aghamohammadi^{1†}, Anton Fernández¹, Malte Schmidt¹, Ana Pérez-Rodríguez¹,
Alejandro Rodolfo Goñi^{1,2}, Jorde Fraxedas^{3,4}, Guillaume Sauthier³, Markos Paradinas¹,
Carmen Ocal¹ and Esther Barrena^{1*}*

¹ Instituto de Ciencia de Materiales de Barcelona (ICMAB-CSIC), Campus de la UAB, 08193
Bellaterra, Spain

² ICREA, Passeig Lluís Companys 23, 08010 Barcelona, Spain

³ ICN2 – Institut Català de Nanociència i Nanotecnologia, Campus UAB, 08193, Bellaterra
(Barcelona), Spain

⁴ CSIC - Consejo Superior de Investigaciones Científicas, ICN2 Building, 08193 Bellaterra
(Barcelona), Spain

ABSTRACT

We address the impact of the relative orientation between donor (D) and acceptor (A) molecules at the D/A heterojunction on the exciton dissociation. For this purpose, two-dimensional heterojunctions of diindenoperylene (DIP) and N,N'-dioctyl-3,4,9,10-perylene tetracarboxylicdiimide (PTCDI-C₈) deposited onto SiO₂/Si are grown, which exemplify two model interfaces with the π -stacking direction either perpendicular or parallel to the interface. Aspects related to the morphology of the heterojunctions and charge photogeneration are studied by scanning probe force methods and photoluminescence (PL) spectroscopy. Results from PL spectroscopy indicate that the exciton dissociation is influenced by the different relative molecular orientations of A and D. For the configuration with stronger orbital overlap between A and D at the interface, the exciton dissociation is dominated by recombination from an interfacial charge transfer state.

KEYWORDS

Organic interface

Scanning probe microscopy

Kelvin Probe Force Microscopy

Photoluminescence

Morphology

Charge transfer state

Introduction

Organic photovoltaic (OPV) devices have been subject of extensive research and development over the past decade. In spite of the progress in the field, with record power conversion efficiencies already beyond 12%,¹ the basic mechanism of photovoltaic generation of free charges is surprisingly not well understood and is being currently debated.²⁻⁴

In organic solar cells, absorbed photons lead to bound electron-hole pairs, or singlet excitons. To contribute to the photogenerated current, an exciton must first be dissociated into free charges. The interface between a donor (D) and an acceptor (A) material, so called D/A heterojunction, has become the fundamental element of organic photovoltaic devices. When an exciton reaches the heterojunction, it can be separated into an electron at the acceptor side and a hole at the donor side if the difference of energy between the lowest unoccupied molecular orbitals (LUMO) of A and D (energy offset) exceeds at least the exciton binding energy. However, variations in photoconversion efficiency for different materials combinations cannot in all cases be explained by this simple energy-level offset picture. Additionally, differences in the electronic structure of the heterojunction, determined by specific features of intermolecular overlap, seem to play a critical role.^{5,6} Several studies have revealed the relevance of charge transfer (CT) states in which the electron at the acceptor side and the hole at the donor side remain bound by Coulomb attraction.⁷⁻¹⁰ This bound electron-hole pair at the interface can either dissociate into free charges or recombine back to the ground state. The interfacial CT state may not only be of high importance for the open circuit voltage of organic photovoltaic devices but also for the extracted photocurrent.¹¹⁻¹² As the wave function overlap at the D/A interface determines the CT properties, the morphology of the heterojunction is expected to have strong influence on the mechanisms of exciton dissociation and recombination. Identifying the specific role of the molecular properties

of D/A interface in thin films poses enormous challenges because thin films contain heterointerfaces with polycrystalline (and often undetermined) structure. This issue has been addressed in several works from a theoretical standpoint.^{5, 13-16} For instance, Verlaak et al. modeled the pentacene/C60 crystalline interface and concluded that both the vacuum-level shift and exciton dissociation critically depend on the orientation of the pentacene π -orbital with respect to the adjacent C60.¹³

In this work we assess experimentally the impact of the relative molecular orientation at D/A interfaces on the exciton dissociation. Our strategy is to grow two nanoscale D/A heterojunctions as model heterointerfaces in which the π -stacking direction is either nearly perpendicular (figure 1a) or parallel to the interface (figure 1b). We have chosen DIP (diindenoperylene) and PTCDI-C₈ (N,N'-dioctyl-3,4,9,10-perylene tetracarboxylicdiimide) as donor and acceptor materials, respectively. DIP is known to exhibit remarkable crystallinity and charge-transport properties¹⁷ and was recently used as donor material with high open-circuit voltage (V_{OC}) in combination with C60.¹⁸ PTCDI-C₈ also exhibits well-ordered thin films,¹⁹ high electron mobility in organic field effect transistors²⁰ and has been used as acceptor material in solar cells with pentacene.²¹ Both molecules, DIP and PTCDI-C₈, are planar conjugated molecules, which grow in an upstanding orientation on weakly interacting surfaces such as SiO₂. Such anisotropic crystalline structure facilitates the study of ordered and well-defined interfaces.

The two relevant phenomena of charge photogeneration and reduced singlet exciton recombination (photoluminescence quenching) have been studied by Kelvin probe force microscopy (KPFM)²² and photoluminescence (PL) spectroscopy. The occupied energy levels of the heterojunctions have been characterized by Ultraviolet photoelectron spectroscopy (UPS).

We successfully provide a clear identification of molecular orientation as one of the factors governing recombination through interface states.

Experimental methods

All samples were fabricated by highly purified material sublimation in ultra-high vacuum (UHV) ($\approx 10^{-8}$ mbar) onto native SiO₂/Si (p or n doped). The substrates were previously cleaned by successive sonication in acetone and ethanol (each 5 minutes), transferred to the UHV chamber and annealed at a temperature of $\sim 300^\circ\text{C}$ (20 minutes). The temperature of the substrate was selected to optimize each growth in order to create the desired heterojunction architectures (horizontal or vertical). Atomic force microscopy (AFM) data were obtained with a commercial instrument from Nanotec Electrónica and analyzed with the WSxM software.²³ KPFM measurements were performed at room temperature in the dark and under illumination using conductive probes (Pt/Cr coated Si tips) mounted in cantilevers with nominal force constant of ~ 2.8 N/m. Topography and lateral force images were measured in contact mode using AFM probes with nominal force constant of ~ 0.1 N/m. All contact mode measurements were performed with the lowest practicable load (close to pull-off force) to avoid damage of the organic layers. PL was measured with a green line of an argon laser (514 nm). Both KPFM and PL measurements were performed under N₂ atmosphere (relative humidity < 5%) to reduce relative room humidity impact. UPS experiments were performed using a PHOIBOS150 hemispherical analyzer with monochromatic HeI (21.22 eV) radiation using n-type silicon with its native oxide as substrate.

Results and Discussion

The substrate of choice is native SiO₂/Si because the thin SiO₂ layer (typically of ~1.5 nm) decouples electronically the molecules from the Si and allows uniform layered growth of films with the molecules in a nearly upright standing orientation. Characteristics of the growth and microstructure of DIP and PTCDI-C₈ can be found in the literature.^{17,19,24-27} In order to have well-defined D/A heterointerfaces, our strategy has been the growth of two-dimensional (2D) islands, i.e. submonolayer coverage. Two types of nanoscale heterojunctions have been grown in a controlled manner: single-component islands of A(D) either nucleated on top (vertical configuration) or side by side (horizontal configuration) of single-component islands of D(A), as schematically illustrated in Figures 1a and 1b, respectively. These two types of heterojunctions exhibit fundamental differences in the structural and electronic properties of the D/A interface, owing to the different relative orientation of the π -molecular orbitals in adjacent DIP and PTCDI-C₈ molecules and to the changed distance between the center of their molecular cores. Thus a stronger electronic coupling is expected for the horizontal configuration (figure 1b) due to overlap of the π -orbitals of neighboring DIP and PTCDI-C₈ molecules across the D/A interface.

The lateral dimension of the 2D islands can be tuned by appropriate selection of both substrate temperature and coverage while keeping the coverage under the complete monolayer (ML). Figure 2a and 2b show the topography and corresponding lateral force signal of DIP islands covering ~54% of the surface (i.e. 0.54ML). The measured island height is ~1.7 nm (see line profile in Figure 2c) in agreement with the standing upright orientation of the first layer of DIP determined in previous studies.^{27,28} Islands of PTCDI-C₈ can be seen in Figure 2d corresponding to a coverage of ~0.6 ML. The measured height of 2.2 nm (line profile in Figure 2f) agrees with the interlayer distance determined by x-ray diffraction (XRD) that corresponds to a tilted

orientation of PTCDI-C₈ molecules.^{19, 25} In both cases, the islands of DIP and PTCDI-C₈ are distinguished from the substrate by a darker contrast in the lateral force images (Figures 2b and 2e), due to the lower frictional force sensed by the tip on them as compared to the substrate. The lower friction on PTCDI-C₈ as compared to DIP provides an additional useful tool for identification of the two molecules in horizontal heterojunctions as we will show in the following.

The so-called horizontal heterojunctions were fabricated in a sequential way by an initial deposition of islands of PTCDI-C₈ (or DIP) followed by the subsequent deposition of a submonolayer of DIP (or PTCDI-C₈). This procedure results in the nucleation and growth of DIP around PTCDI-C₈ islands (and vice versa). The structure within DIP and PTCDI-C₈ domains in the horizontal heterojunctions is the same as in pure samples, as revealed by the layer height, the frictional signal and the molecular periodicity. An example of such horizontal heterojunctions is shown in Figure 2g and 2h. Single component domains of each molecule can be distinguished by the height difference in topography (Figure 2g and profile in 2i) and by the contrast of the lateral force image, where darker areas correspond to PTCDI-C₈. The molecular periodicity additionally allows identification of the crystalline domains formed by each molecule. For instance, the lateral force image shown in Figure 3 has been taken by scanning across the line boundary between DIP and PTCDI-C₈ domains in one horizontal heterojunction. Two distinct periodic structures are observed that are characteristic of the molecular order of DIP and PTCDI-C₈, respectively. The pseudo hexagonal periodicity observed for DIP with an average lattice of ~0.6 nm (left-upper part in Figure 3a) corresponds to the nearest-neighbor distance between DIP molecules ordered in a herringbone pattern.²⁹ PTCDI-C₈ exhibits a striped structure with a periodicity of 1.05 nm (Figure 3b) in agreement with the slip-stacked face-to-face arrangement.¹⁹

The measured intermolecular distances are within the experimental error (± 0.1 nm) in agreement with the reported unit cells. The two-dimensional fast Fourier transformations (2D FFT) of the DIP and PTCDI-C₈ structures (Figure 3b and 3c) have been calculated from the respective domains, displaying the underlying symmetry of the molecule arrangement.

The so-called vertical heterojunction (Figure 1a) was also fabricated in a sequential way; in this case by the deposition of PTCDI-C₈ on top of one initial monolayer of DIP. The height of this architecture is ~ 4 nm, corresponding to the added layer heights of DIP and PTCDI-C₈ (Figure 2j,k,l). Compared to the side-by-side arrangement of molecules in the horizontal heterojunctions, the vertical heterojunction implies a different orientation of their π -molecular orbitals and, at the same time, a larger distance between the centers of the aromatic cores. The π -orbital of DIP and PTCDI-C₈ molecules does not overlap in this configuration because, besides their near parallel orientation to the heterointerface, the alkyl chains of PTCDI-C₈ separate their aromatic cores electronically decoupling them. Molecular periodicity, frictional signal and topographical profiles indicate similar molecular packing as for PTCDI-C₈ on SiO₂/Si. Unfortunately, the reverse architecture, i.e. DIP on top of a PTCDI-C₈ layer, was not successfully achieved because DIP molecules intercalated in between crystalline domains of the underlying PTCDI-C₈.

To investigate photoinduced charging phenomena in the grown heterojunctions, we employed KPFM, which allows the characterization of the surface potential (SP) at the nanoscale. The topography and the simultaneously measured SP maps for single-component samples are shown in Figures 4a-4b and 4d-4e, for DIP and PTCDI-C₈, respectively. DIP islands appear brighter than the non-covered surrounding SiO₂ substrate in the SP images, indicating a larger surface potential which amounts to $\Delta_{SP}(\text{DIP-SiO}_2) = 0.06 \pm 0.01$ eV. PTCDI-C₈ islands, on the other hand,

appear darker than the surrounding substrate with a $\Delta_{SP}(\text{PTCDI-C}_8\text{-SiO}_2) = -0.05 \pm 0.03$ eV. Although the origin of the observed SP contrast between the molecular islands and the substrate is not yet fully understood, interfacial dipoles caused by charge transfer between molecules and the silicon substrate can be ruled out by the energetically unfavorable position of the energy levels of DIP and PTCDI-C₈ with respect to the Fermi level of the underlying silicon substrate.^{30,31} Furthermore, similar contrast is observed using either p-doped or n-doped silicon substrates. Although the measurements have been done in a controlled environment to minimize the effect of water adsorption, the samples were transferred through air from the UHV chamber to the KPFM equipment. Therefore, environmental factors (such as moisture, oxygen or/and contaminants) might partly influence the measured SP values.³²

The topography and surface potential maps in horizontal heterojunctions are also shown in Figure 4 for the case of PTCDI-C₈ surrounded by DIP (Figure 4g-4h) and DIP surrounded by PTCDI-C₈ (Figure 4i-4k). The sign of the surface potential for DIP and PTCDI-C₈ is the same as the ones observed in single-component samples but, the difference between DIP and PTCDI-C₈ in horizontal heterojunctions is a few tens of mV larger in some samples, which could be a hint of hole and electron trapping in DIP and PTCDI-C₈, respectively, caused by charge photogeneration due to exposure to ambient light. Indeed, the comparison of KPFM performed in the dark and under wideband illumination in the same surface location, shows slight changes in the distribution and magnitude of the surface potential (Figure SI.1 in Supporting Information). However, since we obtain large variability of $\Delta_{SP}(\text{PTCDI-C}_8\text{-DIP})$ values between samples, the KPFM results cannot be considered as conclusive evidence of photocharging phenomena.

To gain more valuable insight into the effect of the structure of the D/A interface in exciton dissociation, we have carried out PL spectroscopy in both types of heterojunctions and in the single component systems. Figure 5 shows the normalized PL spectra for all four cases. Figures 5b-e show the AFM morphology of the samples for which these particular PL measurements have been performed. The horizontal configuration (figure 5d), consists hereof islands of DIP surrounded by a rim of PTCDI-C₈ and the vertical configuration is made out of 0.8ML of PTCDI-C₈ grown on top of 1ML of DIP (Figure 2). We note that green laser light ($\lambda=514$ nm) is absorbed by both, DIP and PTCDI-C₈.^{18,33} The PL spectrum of DIP shows characteristic well-defined peaks at ~ 575 nm and 625 nm in accordance to previous PL measurements in DIP thin films²⁶, while PTCDI-C₈ shows a broader PL emission centered at around 650 nm. The PL spectrum of the vertical heterojunction shows contributions of the emission of the single components due to recombination from singlet excitons (Figure SI.2 in Supporting Information). In contrast, the PL of the horizontal heterojunction differs drastically in which the appearance of an additional longer wavelength emission peak at ~ 737 nm is remarkable. This is the chiefly pronounced peak dominating the spectrum for the horizontal configuration, while it is only very weak (seen as a shoulder further commented below) for the vertical heterojunction. The observation of a red-shifted broad peak in blends have been reported for different combination of A and D materials and is considered a signature of radiative recombination from a CT exciton to the ground state across the D/A interface.³⁴⁻⁴⁰ The energy of the CT emission estimated from the PL peak observed in the horizontal heterojunction is $E_{CT} \sim 1.7$ eV. Note that this peak appears as a shoulder in the vertical architecture, i.e., much weaker than in the horizontal case (Figure SI.2 in Supporting Information). This observation is most likely due to the existence of some adjacent stacking of DIP and PTCDI-C₈, since taking into account the

error of the quartz crystal monitor, the DIP coverage may differ by $\pm 5\%$ from 1ML and, therefore, contain few pinholes within the layer where PTCDI-C₈ can nucleate in a side by side configuration.

These results show the profound impact of the different relative orientation of D/A molecules at the interface on its electronic properties and hence in the exciton dissociation/recombination mechanisms. Although it is difficult to assess quantitatively from the PL intensities we note a trend of stronger CT emission for larger interfacial area (Figure SI 3).

The energy of the CT state, $E_{CT} \sim 1.7$ eV, can be compared with the difference between the highest occupied molecular orbital (HOMO) of the donor and the lowest unoccupied molecular orbital (LUMO) of the acceptor. The $HOMO_{(D)}-LUMO_{(A)}$ difference is usually defined as the effective band gap of the heterosystem (E_G). The value of the HOMO with respect to the vacuum level, referred to as ionization potential (IP), is $IP_{DIP} = 5.2$ eV for ultra-thin layers of DIP on SiO₂.³⁰ On the other hand, the estimated electron affinity (LUMO with respect to the vacuum level of PTCDI-C₈ is ~ 3.9 eV,⁴¹ giving an estimated E_G of $HOMO_{(DIP)}-LUMO_{(PTCDI-C_8)} \sim 1.3$ eV, which is clearly smaller than the energy of the CT exciton (E_{CT}) and does not seem to be physically reasonable. However the energy band offsets at D/A heterojunctions may differ from the single components cases, even in absence of charge transfer.⁴²⁻⁴⁴ To explore this possibility, we carried out UPS experiments for the same horizontal and vertical heterojunctions in figure 5d and 5e, respectively, and for a submonolayer coverage of DIP for comparison. The UPS spectra are plotted in the figure 6. For the DIP sample the onset of the HOMO is at 1.07 eV below the Fermi-level (EF) of the SiO₂/n-Si substrate (4.1eV below the vacuum level) in excellent agreement with previous reported UPS data.³⁰ For both heterojunctions there is a shift of ~ 0.2 eV of the HOMO towards larger binding energy, with a slightly larger shift for the horizontal

heterojunction. The shift of the HOMO position in the heterojunctions can be attributed to decreased polarization energy, which as reported by Akaike et al., can lower the HOMO and raise the LUMO causing an effective increase of the E_G of 0.2-0.5 eV.⁴² An enlarged E_G in the heterojunctions agrees with an energy picture in which the E_{CT} is similar or slightly lower to E_G .

Conclusions

As a first conclusion of this work, we have shown evidence of an interfacial CT state for the horizontal heterojunction as a direct consequence of the overlap of π -orbitals of neighboring DIP and PTCDI-C₈ molecules across the D/A interface. The second relevant message is that PL from singlet excitons, both in DIP and PTCDI-C₈, is not quenched when the molecules assemble in a vertical configuration. Thus, in spite of the fact that the energy offsets are supposed to be favorable for the exciton dissociation and the larger D/A interfacial area for this architecture, charge transfer across the D/A interface is hindered by the unfavorable orientation of the π -orbitals with respect to the heterointerface and the presence of the insulating alkyl chains.

We provide a clear identification of relative molecular orientation as one of the significant factors governing exciton dissociation through interfacial states and outline the importance of the local structure at the A/D heterojunction for the charge photogeneration processes. The specific local structure of the heterointerface also affects the relative position of the energy levels, which result shifted with respect to the values of the individual materials. The present work states the crucial need of achieving local structural control of organic/organic interfaces by means of molecular design and growth engineering in order to improve the performance of photovoltaic devices.

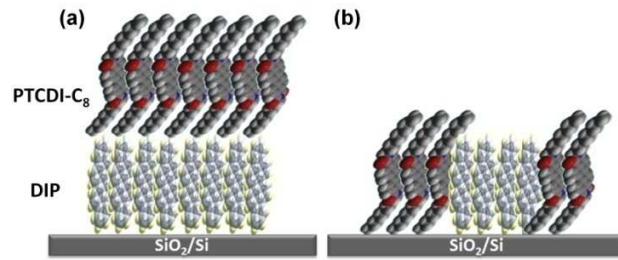


Figure 1. Schematic drawings of the two nanoscale heterojunctions made out of DIP and PTCDI-C₈ grown on SiO₂/Si as model heterointerfaces, referred to as (a) vertical and (b) horizontal.

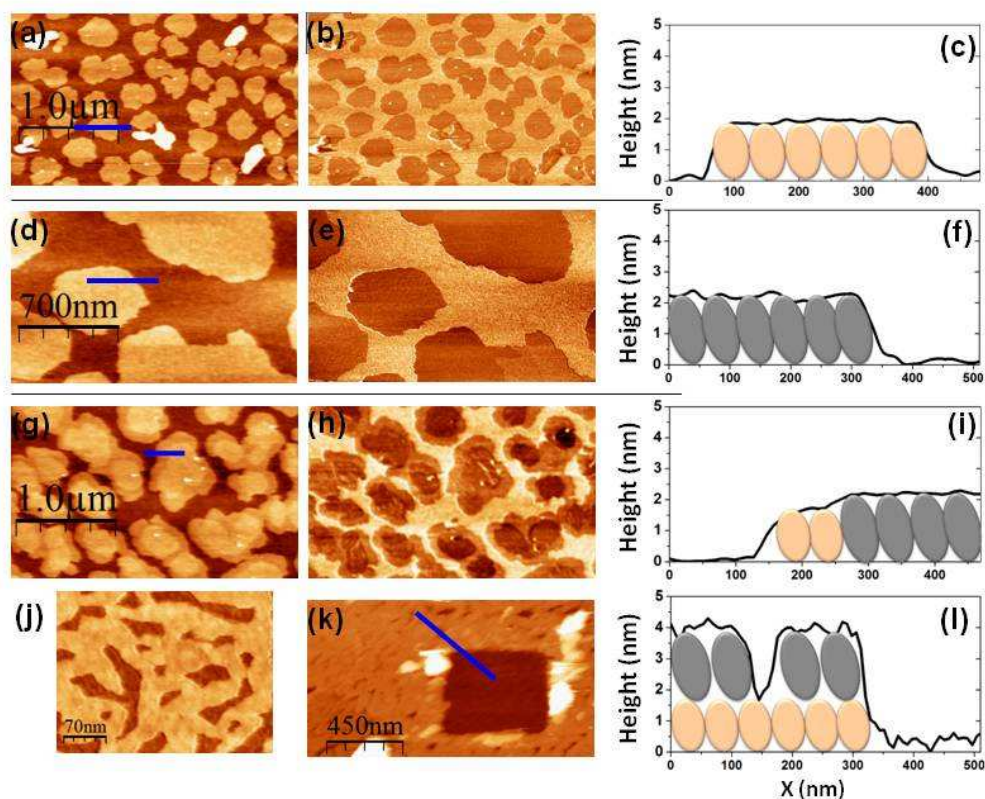


Figure 2. AFM topographic images (contact mode) for single component islands of (a) DIP (d) PTCDI-C₈ and (g) one horizontal heterojunction formed by DIP nucleated around PTCDI-C₈ islands. The corresponding lateral force images (forward) simultaneously acquired are shown in (b), (e) and (h). The lateral force signal (related to the frictional force) provides a means for distinguishing DIP and PTCDI-C₈ domains in the horizontal heterojunctions; PTCDI-C₈ appears with darker contrast (h). Topographic profiles are given in (c),(f) and (i) to illustrate the difference in height between DIP and PTCDI-C₈ islands.(j) Topographic image of vertical heterojunction (PTCDI-C₈grown on top of 1MLof DIP). (k) In order to verify the deposited thickness, molecules have been removed from a squared area by applying a sufficiently high load during the AFM measurement to scratch the organic layer and reach the SiO₂ substrate

underneath. The line-profile in (l) shows the total height of ~ 4 nm of the configuration of PTCDI- C_8 on top of DIP.

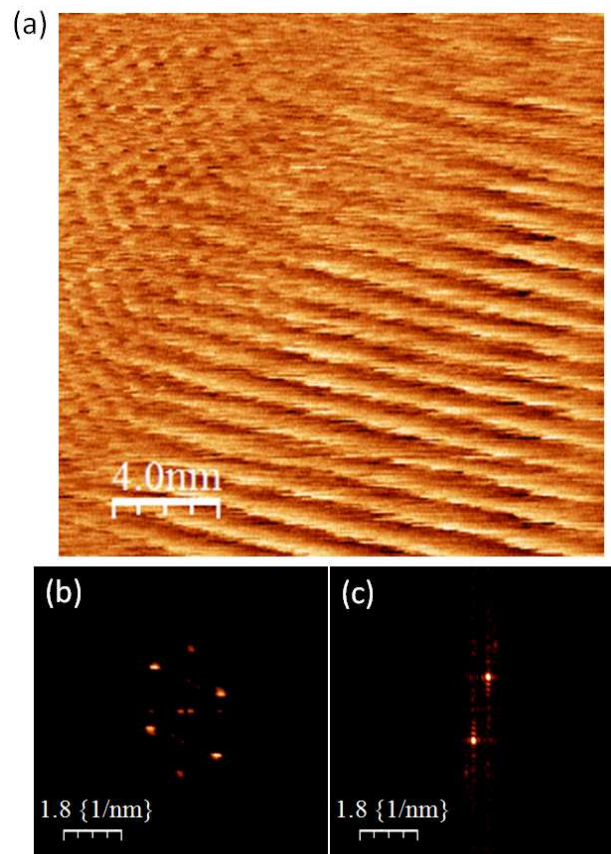


Figure 3.Top: (a) Lateral force image, taken at the domain boundary between DIP (left) and PTCDI- C_8 (right) in a horizontal heterojunction, showing the molecular periodicity at each domain. The periodicity of the molecular structure is revealed, pseudo hexagonal for DIP and striped for PTCDI- C_8 . Bottom: the two-dimensional fast Fourier transform (2D FFT) patterns from corresponding areas of DIP (b) and PTCDI- C_8 (c).

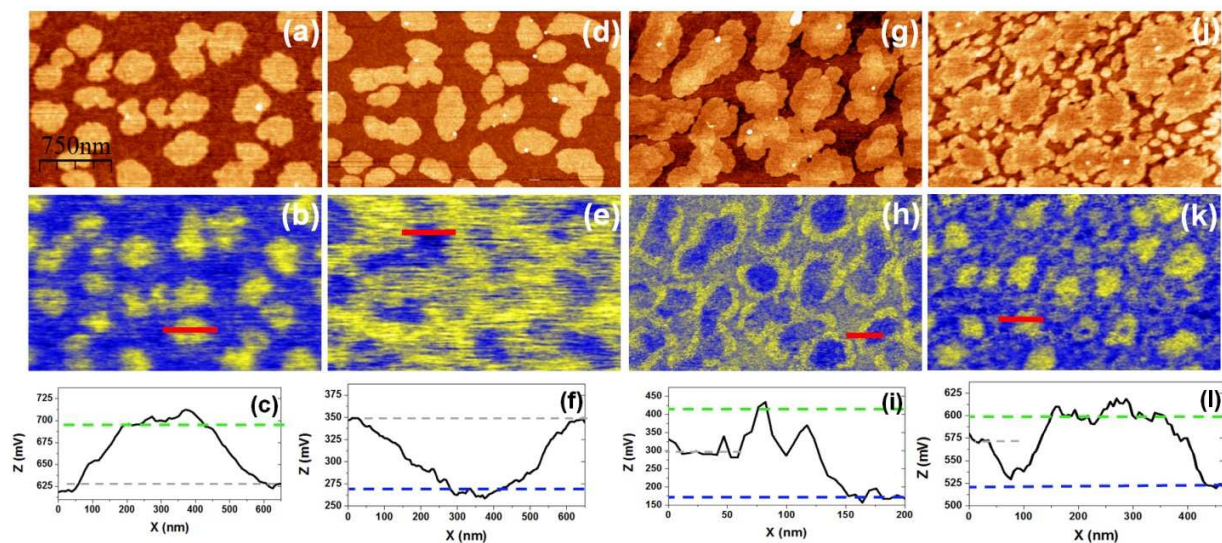


Figure 4. Topographic images (top panels) and surface potential maps (bottom panels) simultaneously acquired by KPFM of (a,b) DIP islands, (d,g) PTCDI-C₈ islands and two horizontal heterojunctions formed by (g,h) DIP nucleated around PTCDI-C₈ islands and (j,k) the reverse case, PTCDI-C₈ around DIP islands. The marked line profiles in the surface potential maps are plotted in (c, f, i, l). In reference to the surrounding substrate (dotted grey line), DIP appears brighter (larger surface potential) (see b) whereas PTCDI-C₈ appears darker (lower surface potential) (see e). For both horizontal heterojunctions (h) and (k), DIP is visible with a larger surface potential than PTCDI-C₈.

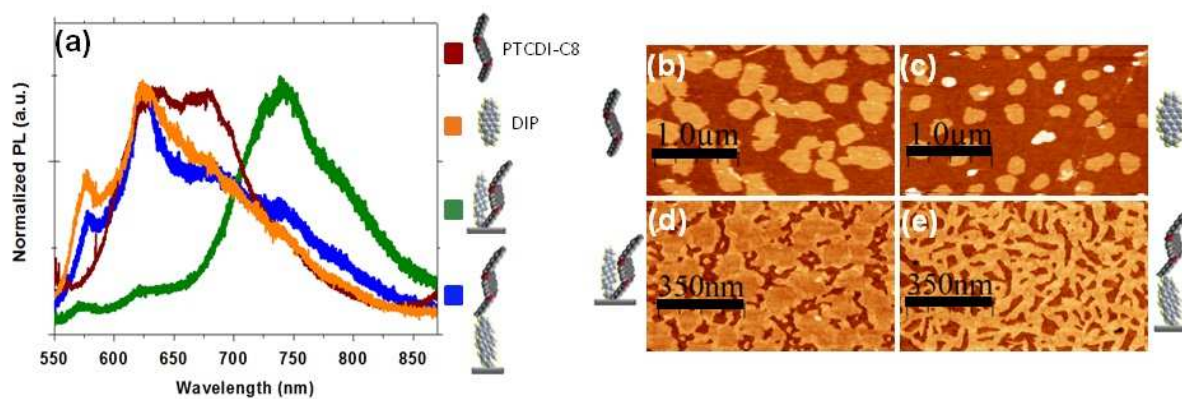


Figure 5.(a) (Color online) Photoluminescence spectra of DIP (orange), PTCDI-C₈ (brown), horizontal (green) and vertical (blue) heterojunctions.(b-e) The corresponding AFM topography images of the samples measured in (a). The horizontal heterojunction (d) corresponds to PTCDI-C₈ nucleated at the edge of DIP islands and the vertical heterojunction (e) to PTCDI-C₈ grown on top of one monolayer of DIP. The emission peak around ~ 737 nm, dominant for the horizontal heterojunction, is assigned to recombination from a charge transfer state.

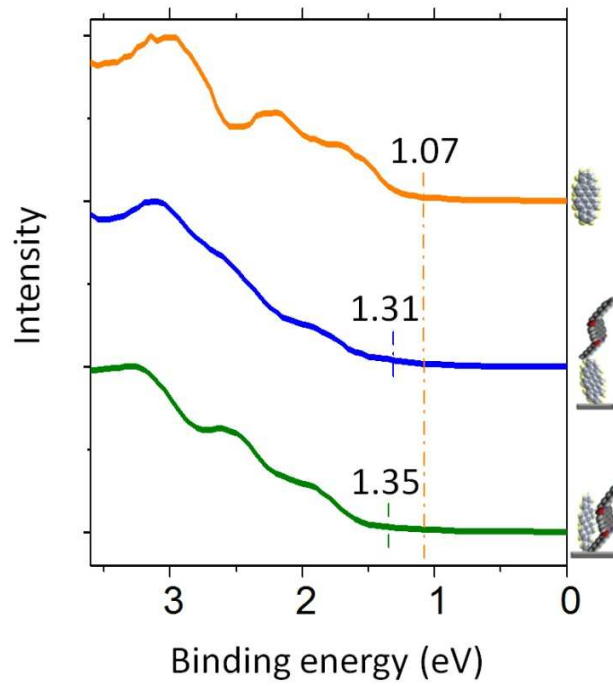


Figure 6.(Color online) UPS spectra for islands of DIP (orange) and for a vertical (blue) and a horizontal (green) heterojunctions. The dashed lines indicate the onset of the HOMO.

ASSOCIATED CONTENT

Supporting Information. KPFM experiment before and after illumination (SI 1), PL of the vertical heterojunction plotted along with the modeled spectral data for PTCDI-C8, DIP and CT, and PL data for other samples (SI 3) are provided in the file with supporting information. This material is available free of charge via the Internet at <http://pubs.acs.org>.

AUTHOR INFORMATION

Corresponding Author

* ebarrena@icmab.es

Present Addresses

†M.Aghamohammadi's present address: Max Planck Institute for Solid State Research,
Heisenbergstr. 1, 70569 Stuttgart, Germany

Author Contributions

The manuscript was written through contributions of all authors. All authors have given approval to the final version of the manuscript.

ACKNOWLEDGMENT

The authors thank Dr.M.Campoy Quiles for fruitful discussions. M.Aghamohammadi would like to acknowledge the members of Organic Electronics group at Max Planck Institute for Solid State Research for their useful inputs and support. Financial support by the Spanish Government (Projects MAT2010-20020 and NANOSELECT CSD2007-00041) and by the German Research Foundation (DFG) within the priority program SPP1355 is acknowledged.

REFERENCES

- (1) Heliatek.Com. http://www.heliatek.com/wp-content/uploads/2013/01/130116_PR_Heliatek_achieves_record_cell_efficiency_for_OPV.pdf (accessed January 16, 2013)
- (2) Vithanage, D.A.; Devižis, a; Abramavičius, V.; Infahsaeng, Y.; Abramavičius, D.; MacKenzie, R. C. I.; Keivanidis, P. E.; Yartsev, a; Hertel, D.; Nelson, J. et al. Visualizing Charge Separation in Bulk Heterojunction Organic Solar Cells. *Nat. Comm.***2013**, *4*, 2334.
- (3) Heeger, A. J. 25th Anniversary Article: Bulk Heterojunction Solar Cells: Understanding the Mechanism of Operation. *Adv. Mater. (Deerfield Beach, Fla.)***2013**, *26*, 1–19.
- (4) Caruso, D.; Troisi, A. Long-range Exciton Dissociation in Organic Solar Cells. *PNAS***2012**, *109*, 13498–13502.
- (5) Huang, Y.; Westenhoff, S.; Avilov, I.; Sreearunothai, P.; Hodgkiss, J. M.; Deleener, C.; Friend, R. H.; Beljonne, D. Electronic Structures of Interfacial States Formed at Polymeric Semiconductor Heterojunctions. *Nat.Mat.***2008**, *7*, 483–489.
- (6) Bakulin, A.; Rao, A.; Pavelyev, V. G.; van Loosdrecht, P. H. M.; Pshenichnikov, M. S.; Niedzialek, D.; Cornil, J.; Beljonne, D.; Friend, R. H. The Role of Driving Energy and Delocalized States for Charge Separation in Organic Semiconductors. *Science (New York, N.Y.)***2012**, *335*, 1340–1344.
- (7) Clarke, T. M.; Durrant, J. R. Charge Photogeneration in Organic Solar Cells. *Chem. Rev.***2010**, *110*, 6736–6767.

- (8) Deibel, C.; Strobel, T.; Dyakonov, V. Role of the Charge Transfer State in Organic Donor-acceptor Solar Cells. *Adv. Mater. (Deerfield Beach, Fla.)* **2010**, *22*, 4097–4111.
- (9) Tvingstedt, K.; Vandewal, K.; Gadisa, A.; Zhang, F.; Manca, J.; Inganäs, O. Electroluminescence from Charge Transfer States in Polymer Solar Cells. *J. Am. Chem. Soc.* **2009**, *131*, 11819–11824.
- (10) Zhu, X.; Yang, Q.; Muntwiler, M.; Charge-, F. Charge-Transfer Excitons at Organic Semiconductor Surfaces and Interfaces. *Acc. Chem. Res.* **2009**, *42*, 1779–1787.
- (11) Vandewal, K.; Gadisa, A.; Oosterbaan, W. D.; Bertho, S.; Banishoeib, F.; Van Severen, I.; Lutsen, L.; Cleij, T. J.; Vanderzande, D.; Manca, J. V. The Relation Between Open-Circuit Voltage and the Onset of Photocurrent Generation by Charge-Transfer Absorption in Polymer : Fullerene Bulk Heterojunction Solar Cells. *Adv. Funct. Mater.* **2008**, *18*, 2064–2070
- (12) Vandewal, K.; Tvingstedt, K.; Gadisa, Inganäs, O.; Manca, J. V. On the Origin of the Open-circuit Voltage of Polymer–Fullerene Solar Cells, *Nat. Mat.* **2009**, *8*, 904 - 909
- (13) Verlaak, S.; Beljonne, D.; Cheyons, D.; Rolin, C.; Linares, M.; Castet, F.; Cornil, J.; Heremans, P. Electronic Structure and Geminate Pair Energetics at Organic–Organic Interfaces: The Case of Pentacene/C 60 Heterojunctions. *Adv. Funct. Mater.* **2009**, *19*, 3809–3814.
- (14) Sreearunothai, P.; Morteani, A.; Avilov, I.; Cornil, J.; Beljonne, D.; Friend, R.; Phillips, R.; Silva, C.; Herz, L. Influence of Copolymer Interface Orientation on the Optical Emission of Polymeric Semiconductor Heterojunctions. *Phys. Rev. Lett.* **2006**, *96*, 117403(1-4).

- (15) Ojala, A.; Petersen, A.; Fuchs, A.; Lovrincic, R.; Pölking, C.; Trollmann, J.; Hwang, J.; Lennartz, C.; Reichelt, H.; Höffken, H. W. et al. Merocyanine/C60 Planar Heterojunction Solar Cells: Effect of Dye Orientation on Exciton Dissociation and Solar Cell Performance. *Adv.Funct.Mater.***2012**, *22*, 86–96.
- (16) Rand, B.P.; Cheyns, D.; Vasseur, K.; Giebink, N.C.; Mothy S.; Yi, Y.; Coropceanu, V.; Beljonne, D.; Cornil, J.; Brédas, J.-L.; Genoe, J. The Impact of Molecular Orientation on the Photovoltaic Properties of a Phthalocyanine/Fullerene Heterojunction. *Adv.Funct.Mater.***2012**, *22*, 2987-2995
- (17) Dürr, a.; Schreiber, F.; Ritley, K.; Kruppa, V.; Krug, J.; Dosch, H.; Struth, B. Rapid Roughening in Thin Film Growth of an Organic Semiconductor (Diindenoperylene). *Phys. Rev.Lett.***2003**, *90*, 016104(1-4).
- (18) Wagner, J.; Gruber, M.; Hinderhofer, A.; Wilke, A.; Bröker, B.; Frisch, J.; Amsalem, P.; Vollmer, A.; Opitz, A.; Koch, N. et al. High Fill Factor and Open Circuit Voltage in Organic Photovoltaic Cells with Diindenoperylene as Donor Material. *Adv.Funct.Mater.***2010**, *20*, 4295–4303.
- (19) Krauss, T. N.; Barrena, E.; Zhang, X. N.; de Oteyza, D. G.; Major, J.; Dehm, V.; Würthner, F.; Cavalcanti, L. P.; Dosch, H. Three-dimensional Molecular Packing of Thin Organic Films of PTCDI-C8 Determined by Surface X-ray Diffraction. *Langmuir***2008**, *24*, 12742–12744.
- (20) Chesterfield, R. J.; Mckeen, J. C.; Newman, C. R.; Ewbank, P. C.; Filho, S.; Bredas, J.; Miller, L. L.; Mann, K. R.; Frisbie, C. D. Organic Thin Film Transistors Based on N-

Alkyl Perylene Diimides : Charge Transport Kinetics as a Function of Gate Voltage and Temperature. *J. Phys. Chem. B***2004**, 19281–19292.

- (21) Rahimi, R.; Narang, V.; Korakakis, D. Optical and Morphological Studies of Thermally Evaporated PTCDI-C8 Thin Films for Organic Solar Cell Applications. *Int. J. Photoenergy***2013**, 2013, 1-7.
- (22) Palermo, V.; Palma, M.; Samori, P. Electronic Characterization of Organic Thin Films by Kelvin Probe Force Microscopy. *Adv. Mater.***2006**, 18, 145–164.
- (23) Horcas, I.; Fernández, R.; Gómez-Rodríguez, J. M.; Colchero, J.; Gómez-Herrero, J.; Baro, a M. WSXM: a Software for Scanning Probe Microscopy and a Tool for Nanotechnology. *Rev. Sci. Instr.***2007**, 78, 013705(1-8).
- (24) Dürr, a. C.; Nickel, B.; Sharma, V.; Täffner, U.; Dosch, H. Observation of Competing Modes in the Growth of Diindenoperylene on SiO₂. *Thin Solid Films***2006**, 503, 127–132.
- (25) Krauss, T. N.; Barrena, E.; Oteyza, D. G. De; Zhang, X. N.; Dehm, V.; Wu, F.; Dosch, H. X-ray / Atomic Force Microscopy Study of the Temperature-Dependent Multilayer Structure of PTCDI-C 8 Films on SiO₂. *J. Phys. Chem. C* **2009**, 4502–4506.
- (26) Heilig, M. Æ.; Domhan, M.; Port, H. Optical Properties and Morphology of Thin Diindenoperylene Films. *J. Lumin.***2004**, 110, 290–295.
- (27) Zhang, X.; Barrena, E.; Goswami, D.; de Oteyza, D.; Weis, C.; Dosch, H. Evidence for a Layer-Dependent Ehrlich-Schwöbel Barrier in Organic Thin Film Growth. *Phys.Rev.Lett.***2009**, 103, 136101(1-4).

- (28) Zhang, X. N.; Barrena, E.; de Oteyza, D. G.; Dosch, H. Transition from Layer-by-layer to Rapid Roughening in the Growth of DIP on SiO₂. *Surf. Sci.* **2007**, *601*, 2420–2425.
- (29) Zhang .X.N., Barrena E., de Oteyza D.G., De Souza E., Dosch H., Growth of Diindenoperylene Single Crystals on Amino-functionalized SiO₂ Surfaces, *J.App.Phys.* **2008**, *104*, 104308(1-4).
- (30) Zhong, J.Q.; Mao, H.Y.; Wang,R.; Qi, D.C.; Cao, L.; Wang, Y. Z.; Chen. W. Effect of Gap States on the Orientation-Dependent Energy Level Alignment at the DIP/F₁₆CuPc Donor/Acceptor Heterojunction Interfaces. *J. Phys. Chem. C* **2011**, *115*, 23922–23928
- (31) Hiroshiba, N. ; Hayakawa, R. ; Chikyow, T.; Yamashita, Y.; Yoshikawa, H.; Kobayashi, K.; Morimoto, K.; Matsuishi, K.; Wakayama Y. Energy-level Alignments and Photo-induced Carrier Processes at the Heteromolecular Interface of Quaterylene and N,N0-dioctyl-3,4,9,10-perylenedicarboximide. *Phys. Chem. Chem. Phys.*, **2011**, *13*, 6280–6285.
- (32) Sergei V. Kalinin and Dawn A. Bonnell, Screening Phenomena on Oxide Surfaces and its Implications for Local Electrostatic and Transport Measurements. *Nanolett.* **2004**, *4*, 555-560
- (33) Karak, S.; Reddy, V.S.; Ray, S.K.; Dhar, A. Organic Photovoltaics Based on Pentacene/N,N-dioctyl-3,4,9,10-perylenedicarboximide Heterojunctions *Org. Electr.* **2009**, *10*, 1006–1010

- (34) Tvingstedt, K.; Vandewal, K.; Zhang, F.; Inganäs O. On the Dissociation Efficiency of Charge Transfer Excitons and Frenkel Excitons in Organic Solar Cells: A Luminescence Quenching Study. *J. Phys. Chem. C* **2010**, *114*, 21824–21832.
- (35) Hallermann, M.; Da Como, E.; Feldmann, J.; Izquierdo, M.; Filippone, S.; Martín, N.; Jüchter, S.; von Hauff, E. Correlation Between Charge Transfer Exciton Recombination and Photocurrent in Polymer/fullerene Solar Cells. *App. Phys. Lett.* **2010**, *97*, 023301(1-3).
- (36) Hallermann, M.; Kriegel, I.; Da Como, E.; Berger, J. M.; von Hauff, E.; Feldmann, J. Charge Transfer Excitons in Polymer/Fullerene Blends: The Role of Morphology and Polymer Chain Conformation. *Adv. Funct. Mater.* **2009**, *19*, 1–7.
- (37) Clark, J.; Archer, R.; Redding, T.; Foden, C.; Tant, J.; Geerts, Y.; Friend, R. H.; Silva, C. Charge Recombination in Distributed Heterojunctions of Semiconductor Discotic and Polymeric Materials. *J. Appl. Phys.* **2008**, *103*, 124510(1-7).
- (38) Anger, F.; Osso, J.O.; Heinemeyer, U.; Broch, K.; Scholz, R.; Gerlach, A.; Schreiber, F. Photoluminescence Spectroscopy of Pure Pentacene, Perfluoropentacene and Mixed Thin Films. *J. Chem. Phys.* **2012**, *136*, 054701-054709.
- (39) Benson-Smith, J. J.; Goris, L.; Vandewal, K.; Haenen, K.; Manca, J. V.; Vanderzande, D.; Bradley, D. D. C.; Nelson, J. Formation of a Ground-State Charge-Transfer Complex in Polyfluorene//[6,6]-Phenyl-C61 Butyric Acid Methyl Ester (PCBM) Blend Films and Its Role in the Function of Polymer/PCBM Solar Cells. *Adv. Funct. Mater.* **2007**, *17*, 451–457.

- (40) Ruani, G.; Fontanini, C.; Murgia, M.; Taliani, C. Weak Intrinsic Charge Transfer Complexes: A New Route for Developing Wide Spectrum Organic Photovoltaic Cells. *J.Chem.Phys.* **2002**, *116*, 1713-1719.
- (41) Jones, B. a; Facchetti, A.; Wasielewski, M. R.; Marks, T. J. Tuning Orbital Energetics in AryleneDiimide Semiconductors. Materials Design for Ambient Stability of N-type Charge Transport. *J. Am. Chem. Soc.***2007**, *129*, 15259–15278.
- (42) Akaike, K.; Kanai, K.; Ouchi, Y.; Seki, K. *Adv.Funct.Mater.***2010**, *20*, 715-721
- (43) Opitz, A.; Wagner, J.; Br, W.; Salzmann, I.; Koch, N.; Manara, J.; Pflaum, J.; Hinderhofer, A.; Schreiber, F. Charge Separation at Molecular Donor – Acceptor Interfaces : Correlation Between Morphology and Solar Cell Performance.*IEEE J.Selected Topics in Quantum Electronics* **2010**, *16*, 1707–1717.
- (44) Fraxedas, J.; García-Gil, S.;Monturet, S.;Lorente, N.; Fernández-Torrente, I.; Franke, K. J.; Pascual, J. I.; Vollmer, A.; Bluhm, R.-P.; Koch N.;Ordejón P. Modulation of surface charge transfer through competing long-range repulsive versus short-range attractive interactions, *J. Phys. Chem. C***2011**, *115*, 18640-18648.

Table of Contents (TOC) Image

